AD_____

GRANT NUMBER DAMD17-93-J-3014

TITLE: Early Detection of Breast Cancer on Mammograms Using: Perceptual Feedback, Computer Processed Images and Ultrasound

PRINCIPAL INVESTIGATOR: Peter Bloch, Ph.D.

CONTRACTING ORGANIZATION: University of Pennsylvania
Philadelphia, Pennsylvania 19104

REPORT DATE: April 1996

TYPE OF REPORT: Final

PREPARED FOR: Commander
U.S. Army Medical Research and Materiel Command
Fort Detrick, Frederick, Maryland 21702-5012

REPORT DOCUMENTATION PAGE

Form Approved
OMB No. 0704-0188

1. AGENCY USE ONLY *(Leave blank)*	2. REPORT DATE	3. REPORT TYPE AND DATES COVERED
	April 1996	Final (31 Dec 92 - 30 Apr 96)

4. TITLE AND SUBTITLE
Early Detection of Breast Cancer on Mammograms Using: Perceptual Feedback, Computer Processed Images and Ultrasound

5. FUNDING NUMBERS
DAMD17-93-J-3014

6. AUTHOR(S)
Peter Bloch, Ph.D.

7. PERFORMING ORGANIZATION NAME(S) AND ADDRESS(ES)
University of Pennsylvania
Philadelphia, Pennsylvania 19104

8. PERFORMING ORGANIZATION REPORT NUMBER

9. SPONSORING/MONITORING AGENCY NAME(S) AND ADDRESS(ES)
Commander
U.S. Army Medical Research and Materiel Command
Fort Detrick, Frederick, MD 21702-5012

10. SPONSORING/MONITORING AGENCY REPORT NUMBER

11. SUPPLEMENTARY NOTES

12a. DISTRIBUTION / AVAILABILITY STATEMENT
Approved for public release; distribution unlimited

12b. DISTRIBUTION CODE

13. ABSTRACT *(Maximum 200* Several approaches for improving the detection of small tumors in the breast were explored. These included; (1) Perceptual feedback to decrease errors in missing tumors that are actually visible on the initial screening mammogram. The observers head-eye-position was recorded while viewing mammograms. It was found that false negative decisions in identifying a lesion was associated with prolonged dwell time. Visual feedback, obtained by placing a small circle on the image surrounding the suspicious region (as predicted by the gaze duration), enhanced the detectability of masses. (2) Computer processing of screening mammograms for detection of clusters of microcalcifications and parenchyma patterns associated with developing lesions. Preserving the high spatial resolution and wide latitude in the digitized mammogram was found important for computer aided detection of subtle microcalcifications. Elevated mammography density has been associated with an increased risk of developing breast cancer. An algorithm was developed to perform quantification of the elevated parenchyma density on digitized mammograms. (3) High resolution ultrasound. The ultrasound distortion in the female breast image were identified and compensating algorithm developed to reduce the distortions. Design considerations were performed for two dimensional large acoustic transducers for high resolution breast imaging. The analysis indicates that using a 2D array would significantly increase the resolution of ultrasound mammography.

14. SUBJECT TERMS	15. NUMBER OF PAGES
Breast Cancer Detection, Biofeedback, Ultrasound, Image Processing	33
	16. PRICE CODE

17. SECURITY CLASSIFICATION OF REPORT	18. SECURITY CLASSIFICATION OF THIS PAGE	19. SECURITY CLASSIFICATION OF ABSTRACT	20. LIMITATION OF ABSTRACT
Unclassified	Unclassified	Unclassified	Unlimited

FOREWORD

Opinions, interpretations, conclusions and recommendations are those of the author and are not necessarily endorsed by the US Army.

N/A Where copyrighted material is quoted, permission has been obtained to use such material.

N/A Where material from documents designated for limited distribution is quoted, permission has been obtained to use the material.

PB Citations of commercial organizations and trade names in this report do not constitute an official Department of Army endorsement or approval of the products or services of these organizations.

N/A In conducting research using animals, the investigator(s) adhered to the "Guide for the Care and Use of Laboratory Animals," prepared by the Committee on Care and Use of Laboratory Animals of the Institute of Laboratory Resources, National Research Council (NIH Publication No. 86-23, Revised 1985).

N/A For the protection of human subjects, the investigator(s) adhered to policies of applicable Federal Law 45 CFR 46.

N/A In conducting research utilizing recombinant DNA technology, the investigator(s) adhered to current guidelines promulgated by the National Institutes of Health.

N/A In the conduct of research utilizing recombinant DNA, the investigator(s) adhered to the NIH Guidelines for Research Involving Recombinant DNA Molecules.

N/A In the conduct of research involving hazardous organisms, the investigator(s) adhered to the CDC-NIH Guide for Biosafety in Microbiological and Biomedical Laboratories.

Peter Glenn 1/31/96

PI - Signature Date

TABLE OF CONTENTS

Early Detection of Breast Cancer on Mammograms Using: Perceptual Feedback, Computer Processed Images and Ultrasound
Peter Bloch, Ph.D., Principal Investigator

FINAL REPORT

Early Detection of Breast Cancer on Mammograms Perceptual Feedback,Computer Processed Images and Ultrasound

Grant # DAMD 17-93-J-3014

Principal Investigator: Peter Bloch, Ph.D.

Clinical data indicates that early detection of breast cancer results in significantly higher success rates in the treatment of the disease. Ten year disease free survival greater than 95 percent are achieved with modern treatment when the breast lesions are detected less than <1 cm in diameter. The goal of this project was to improve the detection of small non-palpable lesions. Three methods for improvement in the detection of small lesions were explored in this study. These include:

Project 1A: Perceptual Feedback as an Aid to the Early Detection of Cancer on Mammograms,
Project 1B: Digital Image Processing of Mammograms, and
Project 1C: High Resolution Ultrasound Mammography.

In summary the major accomplishments include:

- An extensive database of high and low resolution digitized clinical mammograms was established that consists of 87 mammographic examination (two films per study ; a cranial-caudal and a oblique view). The clinical database has pathology confirmed abnormal lesions (34 microcalcifications, 28 masses) and 24 normals. This extensive database was required to test the efficacy of improving detection of lesions on mammograms both by perceptual feedback (project 1A) and computer image processing and feature extraction (project 1B).
- Hardware and software was developed for the computer display of high resolution digitized mammograms
- Elevated mammographic density has been associated in clinical studies with an increased risk of developing breast cancer. Techniques were developed and tested to quantify the fibroglandular tissue automatically from digitized mammograms.
- Algorithms were developed for extracting clusters of microcalcification from the high resolution digitized mammograms
- Hardware and software was developed for recording of eye-position of observers while reading mammograms
- It was found that false-negative decisions in reading mammograms was associated with prolonged visual dwell time. This information was feedback

to the observer (by placing a bold circle around the suspicious site on the image) which resulted in improved detection of masses.

- Two-dimensional ultrasound breast data was obtained and analyzed.
- Ultrasonic distortion in the female breast was identified in the 2D dataset including :(1) phase,(2)incoherent scatter and (3)multipath interference.
- Contrast resolution in breast ultrasound imaging was shown to be significantly restored using a phase deabberration algorithm
- Time-delay type compensation algorithms were developed and found to minimize the scattered energy significantly (15 dB)
- Significant progress was made in recognizing true targets from false ones caused by ultrasound interference. We demonstrated that the image of true targets remains in the same position and changes little in size or shape when imaged from different array locations.
- Design consideration was performed for 2D large acoustic transducers for high resolution breast imaging. The analysis indicated that the ultrawideband property of a 2D array would be more desirable than the conventional narrowband array. This would result in fewer array elements and much lower side band scattered energy .

The achievements on these projects are presented in this final report.

Grant # DAMD17-93-J-3014

Project 1A: Perceptual Feedback as an Aid to the Early Detection of Cancer on Mammograms.

Project Director Harold L. Kundel, M.D.

INTRODUCTION: RESEARCH OBJECTIVES

About 15% of tumors that are actually visible are missed on the initial reading of screening mammograms [Bird et al. 1992]. These misses are considered to be perceptual errors. Eye-position recordings made during the search for tumors on chest radiograms and mammograms have been used to classify perceptual errors into those due to incomplete scanning (15%), failure of the feature recognition mechanism (15%) and incorrect decisions (70%). Decision errors are associated with prolonged visual dwell on the tumor site in the image [Kundel et al. 1989]. Two observations have been made using chest radiograms. First, when sites that receive prolonged visual dwell during primary reading are identified and marked by circling, immediate re-evaluation results in an improvement in accuracy [Kundel, et al.,1990]. Second, circling a tumor site increases the readers ability to detect a tumor [Krupinski et al.,1993].

This project will extend the observations made on chest radiograms to mammograms. The following methodology is being followed. (1) Develop a computer display for mammograms that matches the grayscale properties of the display to the contrast discrimination function of the observer's eye. (2) Interface a head-eye-position recording system to the display. (3) Develop and digitize a set of mammograms with barely visible visual cues for tumor. (4) In a case-control study, compare detection performance with and without eye-position feedback.

PROGRESS REPORT:

Evaluation of the Performance of the Mammogram Display Station

The mammography display station has been implemented using a SUN SPARC 10, Dome video controller boards and two, Tektronix GMA 201 monitors. The active display area is 26 x 26 cm with a pixel matrix of 2048 x 2048 x 8. The images are stored in a 16 bit buffer that is reduced in size (2048 x 2048 pixels) and driving intensity (8 bit) for display. The images can be viewed in reduced size, natural size, and magnified. Reduction is sometimes necessary to fit an entire breast image into the window. Magnification is limited by the available pixels in the display buffer. No pixel replicating is permitted. The monitor gray scale has been perceptually linearized [Blume et al.,1993]. The portion of the intensity range that is displayed over the 8 bit display range is determined by adjusting the intensity window width and window center.

The display was tested using a set of 87 mammograms assembled by Dr. Orel. The set consisted of 34 cases with validated microcalcifications without masses, 28 cases with validated masses without microcalcifications and 25 case matched, control images. The matching of controls is by age, sex, and major incidental image features. The validity

of the normal images was determined by stability of the image findings for at least two years prior to the test mammogram. The images were digitized with two digitizers. Digitizer A (Lumisys) had a nominal scanning spot size of 100 microns and produced a 2030 x 2540 x 12 bit image from a 20 x 25 cm mammogram. Digitizer B (DBA) had a nominal scanning spot size of 43 microns and produced a 5075 x 6350 x 16 bit image from a 20 x 25 cm mammogram. The images were read by three experienced mammographers on film, and on the display station. The readers responses were recorded using a 5 level rating scale format which is consistent with the receiver operating characteristic (ROC) analysis. The data were analyzed using ROCFIT [Metz,1986] and the area under the ROC curve Az determined for the detection of masses and calcification and for the classification of masses and calcification as benign or malignant. The results of the original test (R1) and a replication of the test (R2) made after a lapse of six months are shown in the Table 1.

Table 1. The performance of three readers given as the area under the ROC curve, Mean (St.Dev.).

		Detection		Classification	
		Calc'n	Mass	Calc'n	Mass
Film	(R1)	.98 (.02)	.95 (.03)	.82 (.06)	.77 (.08)
Scanner A	(R1)	.91 (.04)	.92 (.04)	.76 (.09)	.75 (.09)
	(R2)	.91 (.05)	.87 (.07)	.85 (.07)	.63 (.15)
Scanner B	(R1)	.91 (.07)	.93 (.04)	.62 (.10)	.76 (.10)
	(R2)	.87 (.09)	.90 (.05)	.75 (.10)	.75 (.10)

The data indicate that the digitizer-display combination degrades the detection of microcalcifications (The difference of .07 is significant, $p < .05$) but not the detection of masses. Classification shows more variation (.62 to .85 for calcification and .63 to .76 for masses) but is not affected by digitization and soft copy display. This sample could not show a difference between digitizer. The limitation may be in the display.

Confirmation that Gaze Duration Predicts the Location of Tumors by Eye-position Recording During Search

The Applied Science Laboratories (ASL) eye and head position monitor has been used to record the eye-position of 3 mammographers during the search for tumors. We have confirmed the observation that false-negative decisions are associated with prolonged visual dwell time. (This also has been confirmed independently by Krupinski and Nodine [1994].) The ASL eye and head tracker has an accuracy of .5 degrees (.5 cm at 57 cm viewing distance) and a precision of .3 degrees. This means that 95% of x,y coordinates are within .3 degrees of the recorded value (precision) and that 95% of the recorded values are within .5 degrees of the location of the fixation. This level of precision and accuracy is adequate for identifying image sites that receive long visual dwell.

Observations on the Method for Providing Visual Feedback

Visual feedback is provided by putting a five degree circle around the suspicious site. Krupinski et al. [1993] observed that the circle itself increased the detectability of lung tumors. We performed two experiments to study the effect of using a bold circle as a visual prompt.

The first experiment used a background of gausian noise containing a 1 cm object that simulated a mass on a mammogram. Three observers participated in a two alternative forced choice (2AFC) task to measure the detectability of the mass as a function of contrast. The index of detectability d' was measured using standard signal detection procedures. The mass was always displayed in the center of a defined field with a uniformly noisy gray background. Two conditions were compared: the uniform field and the field containing a bold 5 degree circle. The results in the graph below show that the circle enhanced detectability.

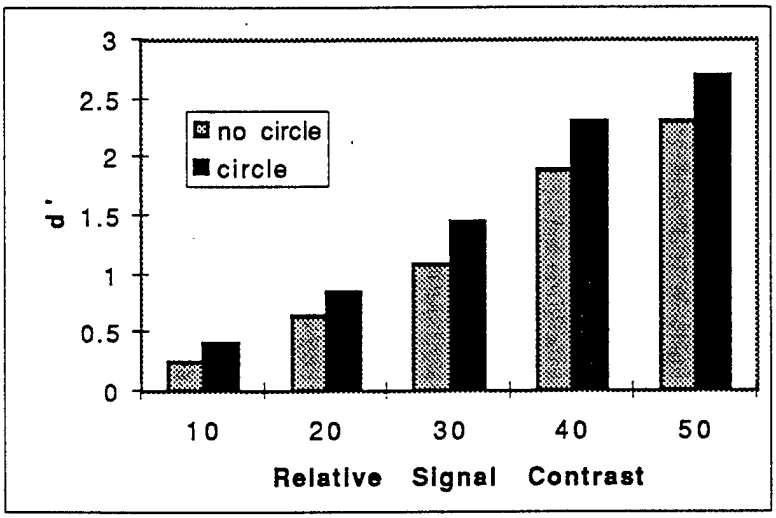

The second experiment used a section of a mammogram as the background in addition to the same level of gausian noise as was used in the first experiment. The results show that the addition of the mammogram as a background decreases the detectability at the two contrast levels and that the addition of a bold circle to the display enhances the detectability.

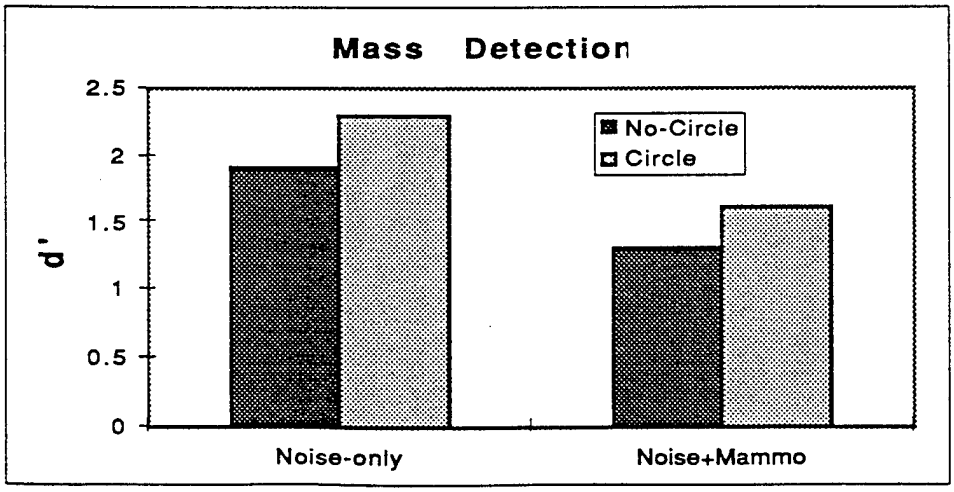

We hypothesize that the circle acts as a fiducial marker for the visual scanning system allowing stabilization of visual drift which has the effect of increasing the contrast sensitivity of the retina [Kundel, 1995]. Data to test this hypothesis has been collected but has not been fully analyzed.

Comparison of Detection Performance With and Without Perceptual Feedback

The eye-position recording system is functioning in a satisfactory manner. We and others have shown that areas containing masses on mammograms receive prolonged visual dwell even when they are not reported. We also have show that a 5 degree bold circle placed on the image enhances the detectability of masses embedded in gausian noise and in breast parenchyma. It now remains to couple the two phenomena in real-time, in order to demonstrate that computer assisted visual search improves performance. This portion of the experiment will be completed as funding becomes available.

SUMMARY

We have developed a system for providing visual feedback in response to measurement of gaze duration during the viewing of mammograms on a video display. We have shown that the display has satisfactory fidelity and that the precision and accuracy of the eye-position tracker is adequate to provide reliable feedback. The feedback consists of drawing a bold circle of 5 degrees diameter around the suspicious site. The circle has been studied independently as a visual prompt and has been shown to be an effective method for enhancing visual performance. The neurophysiologic reason for the enhancement is under investigation. A practical test of computer assisted visual search is being planned.

PUBLICATIONS AND ABSTRACTS

Kundel HL, Nodine CF, Orel SG, Barudin JL, Toto L. Computer assisted visual search in mammography. Radiology 1994;193(P):475.

Kundel HL, Toto, LC and Lauver, S. Further observations on the k effect. Presented at the Sixth "Far West" Perception Conference. Philadelphia, PA. 13 Oct 1995.

REFERENCES

Bird RE, Wallace TW, Yankaskas BC. Analysis of cancers missed at screening mammography. Radiology 1992;184:613-617.

Krupinski EA, Nodine CF, Kundel HL. Perceptual enhancement of tumor targets in chest x-ray images. Percep & Psychophys 1993;53:519-526.

Krupinski EA, Nodine CF. Gaze duration predicts the locations of missed lesions in mammography. In: Gale AG, Astley SM, Dance DR, Cairns AY, ed. Digital Mammography. Amsterdam: Elsevier, 1994: 399-403.

Kundel HL, Nodine CF, Krupinski EA. Searching for lung nodules : Visual dwell indicates locations of false positive and false negative decisions. Invest Radiol 1989;24:472-478.

Kundel HL, Nodine CF, Krupinski EA. Computer displayed eye position as a visual aid to pulmonary nodule interpretation. Invest Radiol 1990;25:890-896.

Metz CE. ROC methodology in radiologic imaging. Invest Radiol 1986; 21:720-723.

Project 1B: Digital Imaging Processing of Mammography Films.

Project Director: Peter Bloch,Ph.D

Introduction

The treatment of small breast lesions (less than 1 cc in volume) with lumpectomy and definitive radiation therapy results in excellent clinical results with 10 year disease free survival better than 95 %. Thus early detection and treatment of breast neoplasms when the lesions are too small to be palpable is most likely to be effective in sterilizing the tumor (Tabar et al.,1992). Mammography examinations are a proven diagnostic procedure for detecting early breast cancer in asymptomatic women (Moskowitz,1984,Kopans,1984 and Feig,1988).

Despite the documented potential for mammography to result in decreased breast cancer mortality, there is some concern that some segments of the population are not fully benefitting from the examination because of variations in quality and interpretation of the mammograms performed. The radiographic appearance of the female breast differs among women in relation to the amounts of fat and fibroglandular (connective and epithelial) tissue present. Areas of fat are radiographically lucent while fibroglandular tissue are radiographic dense. Many studies have looked at the relationship between mammographic density and the risk of developing breast cancer,and the majority of the studies have found an association between parenchymal patterns and risk of developing breast cancer. A recent meta-analysis confirms the association of increasing risk with increasing percentage of density of the breast (Oza and Boyd,1993 and Warner et.al.,1992). The degree of increased risk associated with elevated density may be greater than any other generally recognized risk factor for breast cancer,with the exception of the presence of the BRACA1 gene (Oza and Boyd,1993).

A subjective evaluation of parenchymal density on mammograms, the Wolfe classification scheme (Wolfe,1976), was used for many years,however interobserver variability was a significant problem (Moskowitz et.al.,1980,Myers et.al.,1983,and Carlisle et.al.,1983). It is widely assumed that the sensitivity of mammography is lower in women with increased mammographic density,but the magnitude of the decrease sensitivity has not been studied. This is partially due to the lack of a quantitative measure of mammographic density. A computer assisted method for quantifying mammographic density as a percentage of the image area can overcome this limitation (Boyd et.al.,1995 and Byng et.al.,1994). One of the goals of this research project was to use computer techniques to quantify stromal or parenchymal patterns on mammograms.

Characterization of the breast parenchyma involves analyzing the diffuse mammographic density pattern which depends on the low frequency components in the mammography image. Tumors of diffuse histology are more difficult to detect in the presence of increased mammographic density (Kopans,1992),thus breast density may be the primary cause of missed carcinomas (Kopans,1992 and Hollingsworth et.al.,1993). Estimates of the number of women with mammographically dense breast varies between

10-35 percent (Kopans,1992),decreasing with age. For example,Wolfe et. al.(1987),showed that 66% of women over 53 years old had less than 25% parenchyma density compared to 37% of younger women in that category. Computer identification and processing of mammographic dense mammograms could be an important tool for reading these difficult mammographic cases.

Another goal of this research project was to improve the detectability of breast lesions using computer assisted identification of clusters of microcalcifications on mammograms. Clusters of microcalcification on mammograms is a radiographic feature often identified in early stage breast cancer (Sickles,1986). Approximately 30-50% of the breast carcinomas are detected by microcalcification on mammograms and 60-80% of biopsied confirmed breast carcinomas show microcalcification on histopathology samples. Thus reliable identification of small clusters of microcalcification is a major importance in screening women for early stage disease. Research groups are developing computerized techniques for identifying microcalcifications on mammograms (Chan et al.,1987,1988,1992,Fam et al.,1988,Davies and Dance 1990). Studies from the University of Chicago report 85 percent true microcalcification identification on mammograms using computer-aided detection (CAD) of microcalcification (Wu et al.,1992,Zhang et al.,1992,and Ema et al.,1993). CAD techniques developed by Zheng et.al.,(1995) using topographic feature analysis also report a false-positive detection rate to 0.18/image or 82% true microcalcification detection. In the above studies the mammograms were digitized at 100-175 microns with 10 bits of dynamic range. To further improve on the computer-aided detection of microcalcification a higher quality,high resolution mammographic film digitizer was employed to preserve the spatial resolution and wide latitude of the original mammography film image.

B: Body : Accomplishments of the Project:

B.1 Digitized Mammography Database

Software and hardware tools for archival and retrieval of high resolution digital mammography images are now available for routine use. The software for rapid display of digitized mammographic images with user selected contrast and magnification has been developed using the Interactive Data Language, IDL, package which is readily transportable to different computer platforms. A database of clinical mammograms was established. Dr. Susan Orel, a mammographer, identified 87 clinical mammograms; twenty-five normals, thirty-four with histopathology confirmed microcalcifications and twenty-eight with solid tissue masses. Each mammogram was scanned twice with two different microdensitometers: (1) Lumisys-100 microdensitometer, using a100 micron pixel size and 12 bit dynamic range and, (2) a DBA microdensitometer with a 42 micron pixel size and 16 bit gray-scale. The digitized images were stored for archival on an optical disk. The size of the database of digitized mammography images is approximately 6 gigabytes.

B.2 Performance Characteristics of Microdensitometers:

The performance characteristics of two microdensitometers; (1) Lumisys-100 employing 100 micron pixels and (2) DBA were evaluated for digitizing mammography films. There characteristics are summarized below.

B.2.1 LUMISYS-100 MICRODENSITOMETER

The microdensitometer employs a 2 mW helium-neon laser beam. Precision mirrors mounted on a precision galvanometer movement is used to sweep a 100 micron light spot across the image plane. The light transmitted through the film is detected with a photomultiplier tube, the signal from which is logarithmically amplified and digitized. Linear regression analysis of the microdensitometer output with optical density is shown in fig. 1. The maximum signal intensity occurs at approximately 2.5 OD, corresponding to a useful dynamic range of 11 bits. However the noise evaluated from the analysis of the relative standard deviation in the output from a region of interest, ROI, of 10,000 pixels increases from approximately 0.3% at 2 OD to 0.9 % at 2.5 OD which further reduces the useful dynamic range of the scanner.

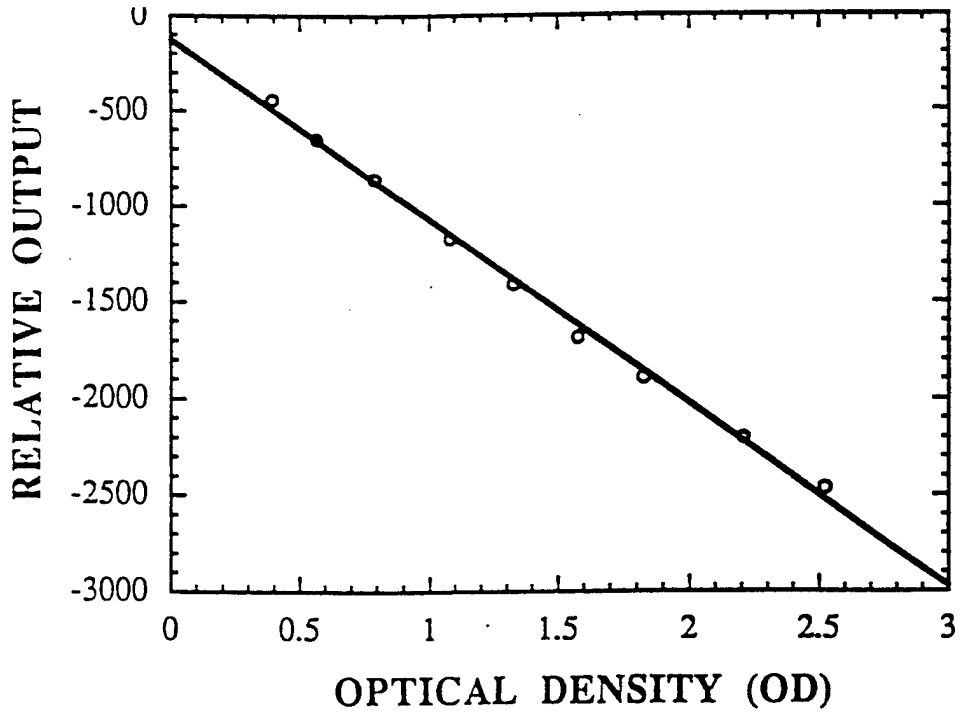

Fig.1: Lumisys microdensitometer output with optical density

The modulation transfer function,MTF,for the microdensitometer was determined by taking the Fourier transform of a line spread function derived from the gradient of a measured edge spread function. The edges of square cut-outs in opaque films, 4 OD, were scanned to measure the edge spread function. The edge spread function was found to be nearly the same for all the edges of the square cutouts. The calculated MTF is shown in fig.2. The highest spatial frequency is the Nyquist cutoff frequency,5 cycles/mm, associated with the 100 micron pixel size.

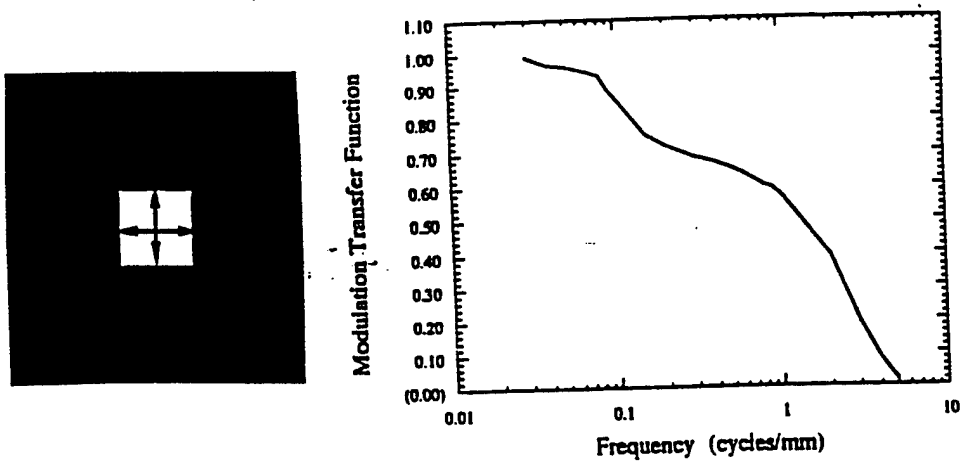

Fig. 2 Modulation Transfer Function for Lumisys Microdensitometer

B.2.2 DBA Microdensitometer

The DBA microdensitometer scans the image plane with a 42 micron wide line light source obtained from a temperature controlled masked straight fluorescent tube. The light is detected with a 6048 linear array charge coupled detector (CCD). An image is digitized by moving the film across the line source. Digitizing a 10x12 inch mammogram requires approximately 22 seconds.

The output of the densitometer is exponential in the optical density range of 0- 4 OD (fig. 3). Routine clinical mammograms contain regions of high density thus the wide range of digitization is important for preserving all the information on the original image.

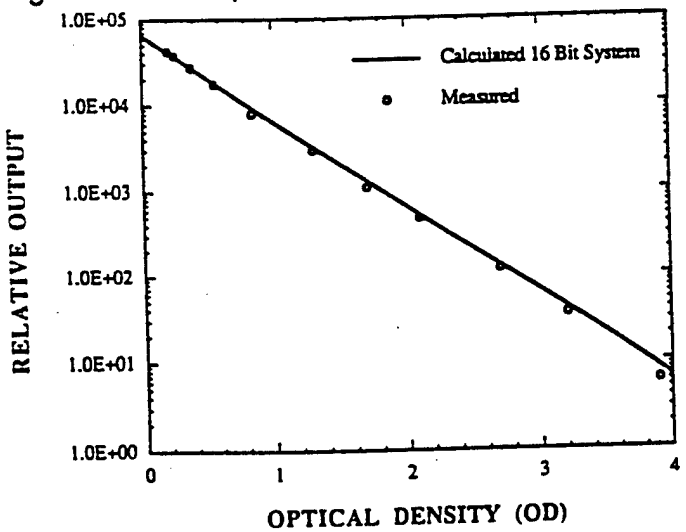

Fig. 3 Output of DBA scanner as a function of optical density

The MTF for the densitometer were derived from the measured edge profile along a single 42 micron wide scan line. The measured edge was found to depend on the edge of the square cutout scanned. Fig. 4 shows that in the direction of the light source the edge is blurred, and sharp in the direction that the film is being scanned. The light in the direction of the line source is scattered, producing glare,whereas in the direction that the film moves the registration of the light source and detectors eliminates the effects of glare.

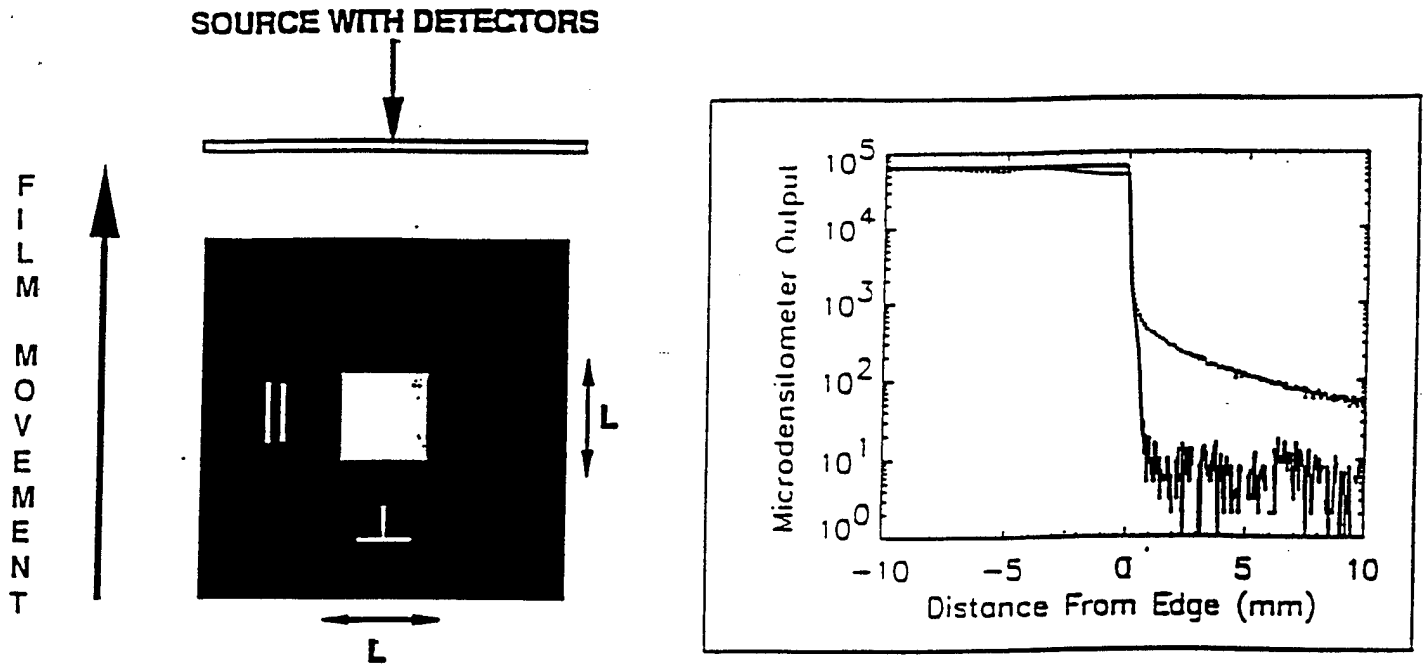

Fig. 4. Edge measured with the DBA microdensitometer. Scanned in the direction of the line light source,(solid line),and perpendicular to the light source (dotted line).

The edge spread function, ESF, in the direction of the line light source was found to be nearly independent of irradiated area, over the range studied 1-25 cm². This area was defined by cutouts in opaque films. In addition, placing neutral density filters between,0.25-0.98 OD, over the square opening did not significantly alter the measured ESF.

The MTF derived for edge spread functions are shown in fig. 5. The high frequency cutoff is at the Nyquist frequency 11.9 cycles/mm corresponding to the pixel size of 42 microns. The MTF at lower frequencies is significantly reduced In the direction of the line source. Thus the degradation in image quality associated with the presence of glare is predominately in the low frequency components. This would suggest that the effects of glare on the image can be significantly reduced by filtering the low frequency components measured in the direction of the light source.

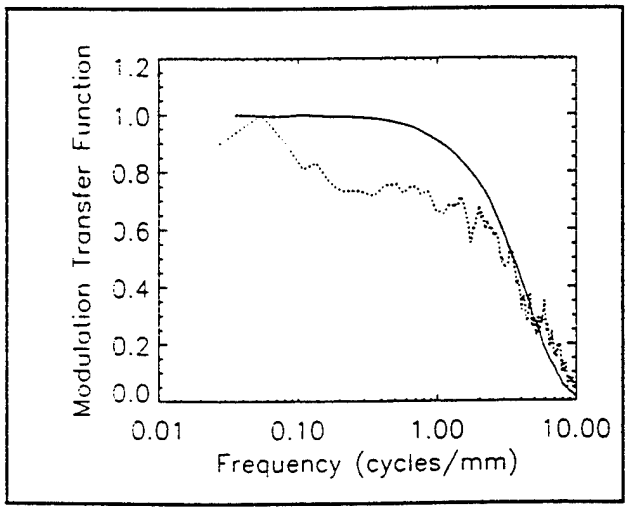

Fig. 5: MTF for the DBA microdensitometer. Scanned in the direction perpendicular to the line light source,(solid line),and in the direction of the light source (dotted line).

Figure 5 indicates that the noise in the direction of the line source is much greater than the noise in the direction perpendicular to the light source. Noise could arise from fluctuations in the; (1) light intensity along the light source, (2) cross talk between elements in the large linear CCD detector array, and (3) analog to digital conversion.

Figure 6 shows the relative noise power spectra measured in three regions: (1) within the square cutout region containing no film, (solid line), (2) in an opaque area lateral to the square cutout in the direction of the line source, (dashed line), and (3) in an opaque area perpendicular to the direction of the line source, (dotted line). In region 2, the noise is associated with glare, which decreases with increasing spatial frequency. In region 3, the noise is a low level white noise. In region 1, superimposed on the noise due to glare is shot noise associated with the linear array CCD detector.

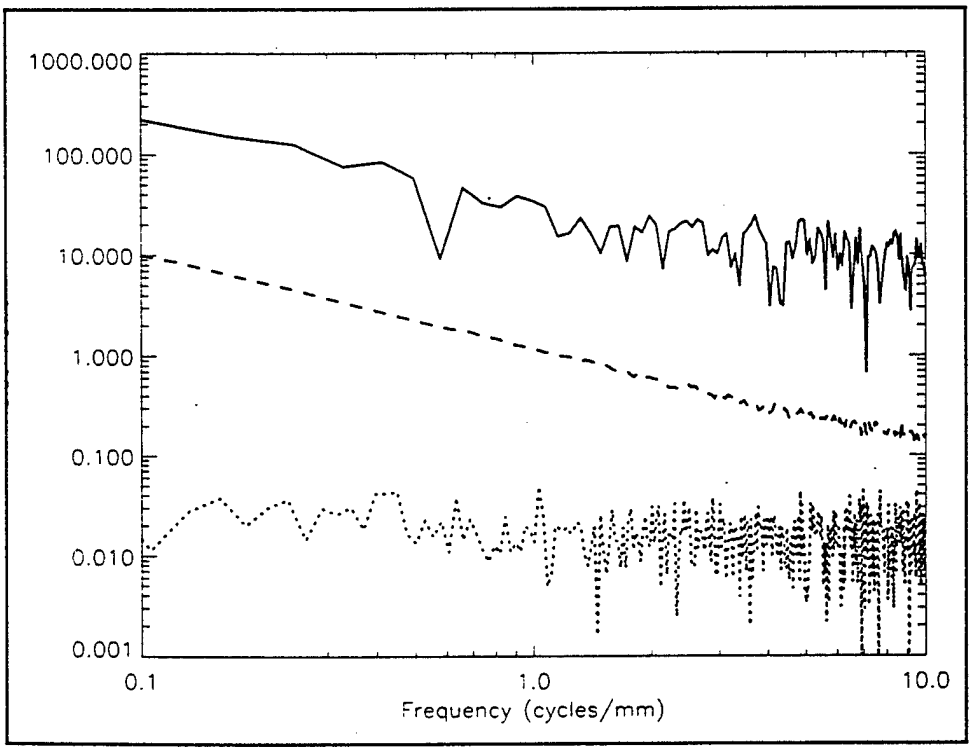

Fig. 6 Relative noise power for the DBA scanner. Solid line, region of high light signal, and opaque regions; (dashed line), lateral to the square cutout in the film in the direction of the light source, and (dotted line) perpendicular to the direction of the linear light source.

The implication of noise on visual perception of microcalcification and masses on digitized images is not clear. However, the directional dependence of the noise may have some implications in computer aided detection,CAD,of clusters of microcalcification. The increase in shot noise associated with the signal intensity may have implication in using CAD for identifying microcalcification in regions of dense breast tissues.

A comparison of the two MTF's in figures 2 and 5 for the Lumisys and DBA scanners respectively demonstrates the improvement in the physical performance of the higher resolution scanner. The results of the observer testing described in project 1B showed however that digitized images produced by both microdensitometers resulted in comparable performance in identifying clustered microcalcifications and masses on mammograms. However, these evaluation did not permit the observer to alter the display contrast. The ability to vary contrast may be a useful tool for the reader in searching for microcalcification in difficult high mammographic density regions of the mammogram (Taylor et al.,1994). The 16 bit digitization depth available with the DBA scanner may be important for preserving the wide latitude of the mammographic film study,however the dynamic range requirements for digital mammography continues to be investigated (Maidment et al.,1993,Neitzel,1994).

Algorithms were developed for identifying clusters of microcalcifications by analyzing the regional distribution in the image of the; (1) power at high spatial frequencies (2) fractal dimension (Lefebvre et al.,1992,1995 and Priebe et al.,1994) and (3) entropy. The analysis used the digitized images obtained with the high resolution microdensitometer.

B.3 Quantitative Determination of Mammographic Density

B.3.1 Background

To quantitate mammographic density, we used the high resolution digitized film set described above. The DBA digitized images were reduced in size to display on a 1k x 1k monitor. We developed software for quantitative analysis of mammographic density based on the method described and validated by Byng et. al. (1994) but with modifications to make the method more operator-independent. To determine the projected area of the breast on the image, the reader selects a background area of approximately 4 x 4 cm2 which contains no breast tissue. The edge of the breast (i_{edge}) is then determined automatically by excluding the region containing all signal less than the mean +4 times the standard deviation of the selected background region. This differs from Byng in that this method requires a knowledgeable observer to select the skin edge of the breast. With our modification, total breast area can be determined by an untrained, naive observer, and is highly reproducible. The total area of the breast is designated A_{br}. The reader then superimposes on the digitized image color computer-generated contour lines of constant signal or optical density and selects the contour line (i_{dens}) that encompasses the region of high mammographic density (Figure 7). The area of increased parenchymal density is equal to the sum of pixels above the threshold (i_{dens}) value designated A_{pd}. The percentage of parenchymal density, PD, is:

$$PD = (A_{pd}/A_{br}) \times 100 \qquad (1)$$

In addition, software has been developed to produce a histogram of signal intensities from the digitized image. The threshold for i_{dens} can be interactively selected by the observer, as described above by Byng et. al.,(1994) and compared with the histogram.

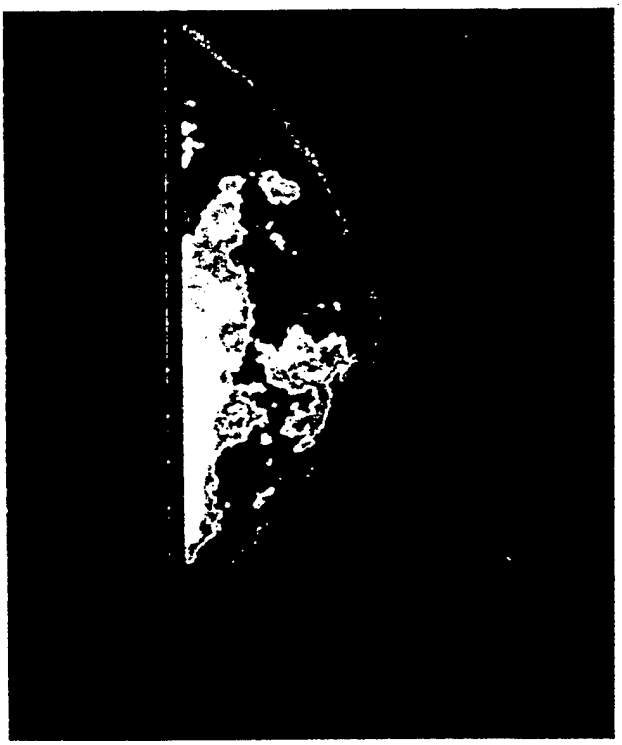

Fig.7. Example of digitized mammogram with computer generated skin edge (i_{edge},red) to determine breast area, and computer generated contour line (i_{dens},yellow) demarcating area of increased parenchymal density.

A typical histogram of signal intensities associated with fatty, low density tissue is shown in Fig. 8 (left panel) . Region 2, above a signal intensity of approximately 250 corresponds to the higher density fibroglandular tissue. The first derivative of the histogram, (dashed line insert in fig.8), often helps to demarcate the start of region 2.

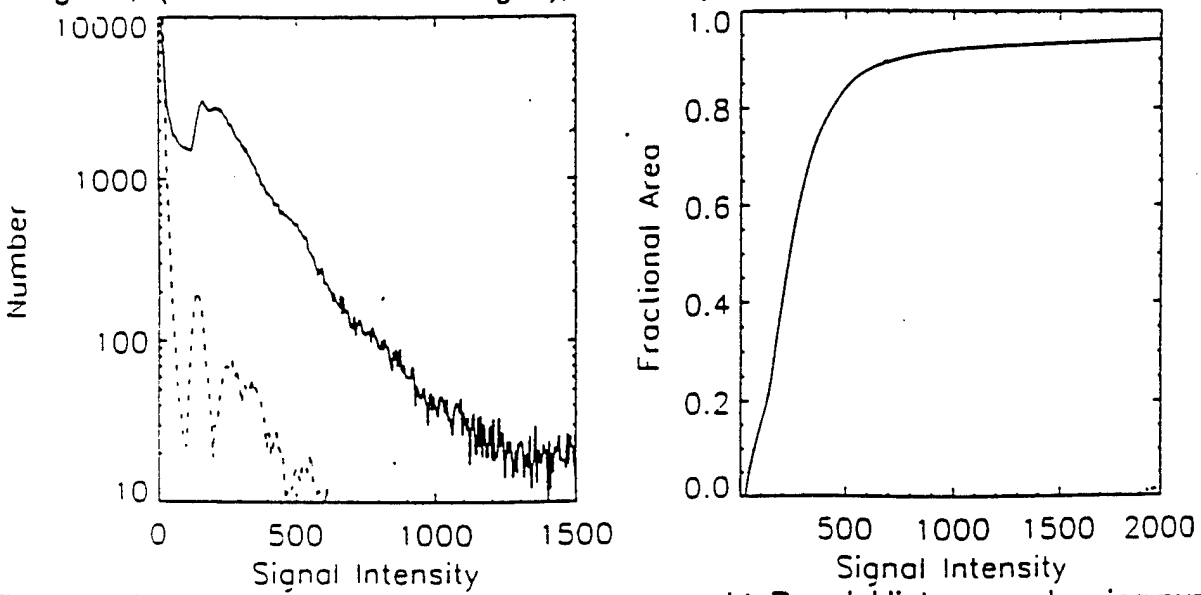

Fig. 8 Analysis of signal intensities in mammogram; Lt. Panel: Histogram showing number of pixels with various intensities (solid line),derivative of histogram(dashed line);Rt. Panel: Fractional breast area-signal cumulative histogram.

The cumulative histogram could also be of use to evaluate the fractional area of the image above a particular signal intensity. A cumulative histogram can be modeled as a sum of normal distributions with different means x(i) and Gaussian spread parameter σ(i) by the integral. The breast tissue area F(ξ) having signal intensity less than ξ is

$$F(\xi) = \int_0^{\xi} \{N(1)\exp-\sigma(1)^{-}(\xi-x(1))^2 + N(2)\exp-\sigma(2)\ (\xi-x(2))^2++++\}d\xi \qquad (2)$$

where N(1) and N(2) are the number of events in peaks x(1) and x(2) respectively. The Gaussian spread parameters can be evaluated from the full-width half-maximum for each peak in the histogram distribution. The fractional area of a mammogram having a signal intensity below a particular level ξ, $F(\xi) / F(\infty)$ is shown in fig. 8 (right panel). As a first approximation the break from the linear portion of the sigmoid curve was used to determine the fraction of elevated density in the image which is 1 - 0.64 = 0.36 or 36% for this example. In practice, however, a least-square-fit to the cumulative histogram is employed to extract the fraction of elevated tissue in a mammogram.

B.3.2 Results of Mammographic Density Analysis

Twenty mammograms from a test set were randomly selected for this preliminary study to demonstrate methods and data analysis of (a) the inter-radiologist reliability of the radiologists' assessments of density; and (b) the concordance between radiologist assessment of density and computer-measured density. The original films were presented independently to 3 radiologists who assigned 1 of 4 subjective categories of density to each case. The 4 categories were: (1) less than 25% high density, (2) 25 to 49% high density, (3) 50 to 75% high density, and (4) greater than 75% high density.

Computer-assisted measurement of high density parenchyma was performed as described above on the digitized images of the same cases. The quantitative measurements were performed by a physicist unfamiliar with interpreting mammograms, assisted by a student research assistant with no mammography experience. The cumulative histograms were used to evaluate the percentage of mammographic area with high density.

1. Table 3 gives mean radiologist assessment (1-4 scale) for each radiologist:

Table 3

Radiologist	Mean	SD
1	2.5	1.1
2	2.8	1.1
3	2.5	1.2

An analysis of variance (ANOVA) model including radiologist and patient number as factors, showed significant differences among radiologists ($p = 0.017$) on this assessment.

The patient terms are needed to control for the correlation induced by having three assessments done on each patient. Essentially, the patient terms force the comparison among radiologists to be made within patient.

2. We calculated the intraclass correlation coefficient (ICC) as a measure of agreement among radiologists. The ICC is defined as the ratio of the among-patient variance in radiologist assessments to the total variance (among-patient and within-patient) in radiologist assessments of density. Because the within-patient variability results from disagreements among radiologists, the ICC provides a measure of agreement. The values of the ICC range from 0 to 1. When there is perfect agreement among radiologists, there will be no within-patient variability, and the ICC would be 1.

We estimated the ICC using an ANOVA model with radiologist assessment as the outcome variable and patient as the grouping factor. The ICC is then calculated as:

$$ICC=BMS / (BMS + (m-1)WMS) \qquad (3)$$

where BMS is the "between" patient mean square form the ANOVA model, WMS is the "within" patient mean square from the ANOVA, and m is the number of measurements on each patient, in this case, 3. The calculated value of the ICC for the data was 0.89, indicating excellent agreement among radiologists. This probably reflects the fact that the three radiologists practice together.

3. Associations between the quantitative measure of density and the radiologists' assessments were evaluated in several ways. For each radiologist individually, and then for all radiologists together, we estimated the Spearman correlation coefficient between the assessment and the quantitative data using the radiologist's assessment as an ordinal predictor variable. Because the regression R^2 values were in nearly perfect agreement with the Spearman coefficients, only the Spearman correlations are presented (Table 4).

Table 4

Radiologist	Spearman Rho
1	0.85
2	0.79
3	0.76
Overall	0.79

These correlations show that there is excellent agreement between the radiologists subjective assessments and the quantitative measurements made by untrained observers. The overall R^2 for the regression described above was 0.64, corresponding to a Pearson correlation of 0.8, again nearly perfectly consistent with the Spearman correlations.

4. Table 5 shows the ranges of quantitative values for each category of the radiologist's subjective assessment, along with the means and standard deviations of the means for each category. The mean was calculated for all assessments at a particular

value, regardless of the radiologist or the patient. In other words, every radiologist's assessment of every patient that was a "1", is included in the summary.

This again shows the string association between the subjective and objective scores, but there is considerable overlap of the ranges of quantitative values between categories of the subjective assessments. Note the range of quantitative values grouped by radiologists into a single category.

Table 5

Radiologist's Assessment	Range of Quantitative value(%)	Mean Quantitative value (%)	SD
1 (<25%)	12.36	18.7	6.7
2 (25.49%)	17-71	38.3	14.5
3 (50-75%)	29-85	54.3	21.5
4 (>75%))	53-85	67.8	11.6

B.4 Computer Aided Detection of Microcalcification

B.4.1 Background

The use of computer aided detection (CAD) of microcalcifications on a mammogram is being extensively explored. No one single image feature,however,by itself has been identified for segmenting a possible microcalcification from normal tissue and image noise. CAD techniques have been developed where the signal to noise ratio of microcalcifications are first enhanced by reducing the high frequency quantum noise,and removing the low frequency structured background from the image. Extraction of image features from these filtered images using local adaptive thresholding procedures in conjunction with artificial neural networks have been successfully employed to achieve a true positive microcalcification detection rate of 80-85% (Chan et al.,1987,1988,1990). CAD techniques developed by Zhang et.al.,(1995) using topographic feature analysis also report a false-positive detection rate to 0.18/image or 82% true microcalcification detection. To further improve on the computer-aided detection of microcalcification a higher quality,high resolution mammographic film digitizer was employed to preserve the spatial resolution and wide latitude of the original mammography film image.

The spatial frequencies in mammography images is greater than 10 cycles/mm with the film-screen combination typically employed. The Nyquist frequency corresponding too 10 cycles/mm requires that the pixel size be less than 50 microns. In the above studies the mammograms were digitized at 100-175 microns with 10-11 bits of dynamic range. Chan et.al,(1994) showed however that detection of subtle microcalcification in mammograms may require much finer resolution e.g. 35 micron pixels. The preservation of the higher spatial frequencies in the digitized mammogram permitted us to explore use of the high frequency components for computer identication of microcalcifications.

B.4.1.1 Feature Extraction from Digitized Mammography Images

The following features within small 5x5 mm² (128x128 pixels) region of interests (ROI) on the mammogram were evaluated; (1) signal intensities (2) power spectrum (3) fractal dimension and (4) entropy.

(1) A histogram of the signal intensities within each ROI is calculated and used to identify pixels within the region with elevated signals that may be associated with microcalcifications. The histogram is used to determine the average signal value within each ROI and the contrast between the individual pixel signal and the average value.The region is flagged as suspicious if a small fraction (0.002) of the pixels in the ROI have a signal intensity that results in a contrast of greater than 5%.

(2) The power spectrum in each ROI was analyzed, using a two dimensional Fourier transform (2DFT). Regions of the mammogram with power at spatial frequencies greater than 2 cycles/mm were flagged as regions that may contain small microcalcifications. In addition, the directionality Θ, of power $P(\upsilon)$ at spatial frequency ν was evaluated with the following expression:

$$\Theta(\nu) = \tan^{-1}\{P_y(\upsilon) / P_x(\upsilon)\} \qquad (4)$$

where $P_y(\nu)$ and $P_x(\nu)$ are the spatial frequency components of the 2D-Fourier transform in the two orthogonal directions x and y. Information on the directionality of the power spectrum is used to help separate ROIs with significant power at high spatial frequencies due to microcalcification from those ROIs that have sharp boundaries between fat and high density parenchyma tissue. The directionality of power associated with clusters of microcalcifications is often isotropic, whereas interfaces between tissue types have a preferred direction.

(3) The fractal dimension (FD) within a ROI is a measure of the irregularity of the signal intensities in the region. A constant or a smooth variation of signal intensities within an ROI would approach a FD of 2, whereas the presence of an abnormality such as microcalcifications on a relatively smooth background of breast tissue would correspond to a rough surface approaching a FD of 3. Fractal analysis has been employed by Lefebvre et.al.,(1995) and Priebe et al.,1994 to identify microcalcifications within small regions of a mammography image. We developed an algorithm to calculate the FD from the variation of the power spectrum with spatial frequency (Ruttimann et.al.,1992). The calculated power spectrum $P(\nu)$ at frequency υ is expressed as a power function

$$P(\upsilon) = a\upsilon^{b} \text{ or } \log(P(\upsilon)) = \log(a) + b\log(\nu) \qquad (5)$$

where a least square fit of log{P(v)} vs log(v) was used to determine the value of b and its associated correlation coefficient. The FD in each ROI was calculated from the absolute value of b by the relationship given by Ruttimann, et al, (1992)

$$FD = 3-(b-1)/2 \qquad (6)$$

Due to the sharp discontinuities associated with microcalcifications, the fractal dimension in regions containing microcalcifications is expected to be both elevated with a larger standard deviation compared to normal tissue.

(4) Entropy is a measure of the disorder within an ROI. Regions containing microcalcifications may be more disordered than a region containing normal parenchyma breast tissue. The first order entropy b_E (Pratt ,1978)in each ROI was evaluated using Shannon's Information Law

$$b_E = -\sum_{b=0}^{L-1} (N(b) / M) * \log_2 (N(b) / M) \qquad (7)$$

where $0 \le b \le L-1$ denotes the quantized amplitude levels, M is the number of pixels in the region, and a base-two logarithm is utilized resulting in the entropy measured in bits.

B.4.1.2 Results of Extraction of Microcalcification on Mammograms

An example is shown in using the above feature extraction algorithms to identify suspicious regions on a mammograms. The original matrix size of the mammogram shown in fig.9 was approximately 3000x5000 X 16 bit which was reduced 5 fold to fit on the display monitor. The analysis was performed using the full data set. The power spectrum was analyzed, using 2DFT, within small regions 5x5 mm² (128x128 pixels) of the mammogram. The total number of regions, ROIs, analysed was 738. Regions with power at spatial frequencies greater than 2 cycles/mm are marked on fig. 9. The DBA scanner used to digitize the mammogram has an MTF of 0.75 at 2 cycles/mm and a Nyquist frequency 11.9 cycles/mm. The 100 micron pixel size used with the Lumisys scanner resulted in an MTF less than 0.4 at the 2 cycles/mm threshold frequency used in this analysis (and zero above 5 cycles/mm). Regions 64 and 106 in fig. 9 are biopsy confirmed microcalcification,region 256 is a lead marker placed on the breast,and regions 172,214,218 are near signal intensity gradients associated with the interface of dense and more usual parenchymal tissue.

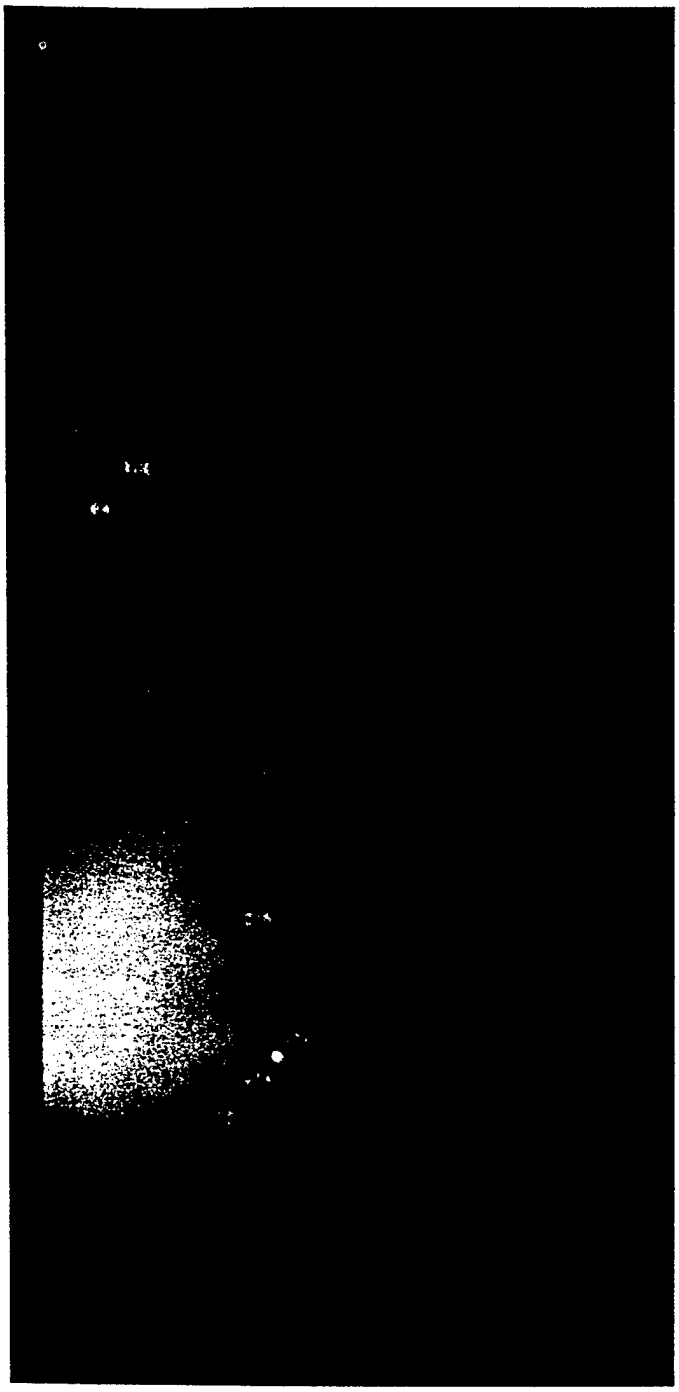

Table 6

Region #	Relative Entropy
64 (μCa)	1.0
106 (μCa)	1.87
172 (tissue interface)	2.56
214 (tissue interface)	3.47
218 (tissue interface)	2.65
256 (lead marker)	4.46

Fig.9 Computer designated suspicious regions on mammogram

Besides the power spectrum the additional image features evaluated in each ROI includes; signal intensity distribution, fractal dimension and entropy. In this example,the most striking difference between the regions with microcalcifications and tissue gradients was in the entropy. Table 6 shows the relative entropy in the ROIs of the image that were flagged. Entropy is a measure of order,the lower the entropy the greater the structure within that region of the image.

B.5 Summary and Accomplishments:

In summary, the goal of the project was to use computer techniques to assist the radiologist in reading mammograms. To accomplish this task, we developed a data base of high resolution digitized mammograms consisting of nearly 100 studies (two views per study). The storage, retrieval, and the processing of these large data files has been shown to be achievable using existing computer technology.

Algorithms were developed during the course of the project to quantify tissue densities on mammograms. The presence of increased mammographic density has been previously identified by radiologists as a primary cause for not detecting carcinomas on mammograms. The ability to quantify parenchymal density mammograms will thus allow physicians to readily separate the "difficult "mammograms for additional study or analysis.

To detect microcalcification on mammograms we developed algorithms that evaluated image features in 5x5 mm^2 regions on the high resolution digitized mammograms. The features that were analyzed include: (1) signal intensity distribution (2) spatial frequency power spectrum, (3) fractal dimension and (4) entropy. The high spatial frequencies preserved in the digitized images helped in computer identifications of microcalcifications. In addition, the disorder in the tissue parenchyma associated with the presence of clusters of microcalcifications can be quantified by evaluating the entropy in the region.

As these findings warrant further studies (particularly observer performance confirmation) we are requesting continuation of the project without any additional funding.

B.6 Literature Cited:

Boyd, N., Byng, J., Jong, R., Fishell, E., Little, L., Miller, A., Lockwood, G., Trichler, D., & Yaffe, M. (1995) Quantitative Classification of Mammographic Densities and Breast Cancer Risk: Results From the Canadian National Breast Screening Study. Journal of the National Cancer Institute, 87(9): p. 670-675.

Byng, J.W., Boyd, N.F., Fishell, E., Jong, R.A., & Yaffe, M.J. (1994)The quantitative analysis of mammographic densities. Phys Med Biol, 39: p. 1629-1638.

Carlisle, T., Thompson, D.J. & Kopecky, K.J. (1983) Reproducibility and consistency in classification of breast parenchymal patterns. AJR, 140: p. 1-7.

Chan, H.P., Niklason, L.T., Ikeda, D.M. et al., (1994) Digitization requirements in mammography: Effects on computer aided detection of microcalcification. Med Phys. 21: p. 1203-1213.

Chan, H.P., Doi, K., Vyborny, C.J., Schmidt, R.A., Metz, C.E., Lam, K.L., Ogura, T., Wu, Y., & MacMahon, H. (1990), Improvement in radiologists' detection of clustered microcalcifications on mammograms. The potential of computer-aided diagnosis. Invest. Radiol. 25: p. 1102-1110

Chan, H.P., Doi, K., Galhorta, S., et al., (1987), Image feature analysis and computer-aided diagnosis in digital radiography.1.Automated detection of microcalcifications in mammography. Med Phys 14: p. 538-548 .

Chan, H.P., Doi, K., Vyborny, C.J., Lam, L. & Schmidt, R.A. (1988), Computer-aided detection of microcalcifications in mammograms: Methodology and preliminary clinical study. Invest. Radiol. 23: p. 664-671

Chan, H.P., Nikalson, L.T., Ikeda, D.M., & Adler, D.D.(1992) Computer-aided diagnosis in mammography: Detection and characterization of microcalcifications. Med Phys 19: p. 831

Ema, T., Doi, K., Nishikawa, R.M. et al., (1993) Computer-aided diagnosis of clustered microcalcification in digital mammograms: Reduction in false-positive findings using edge-gradient analysis. (1993) Radiology Supp. 189: p. 186.

Fam, B.W., Olson, S.L., Winter, P.F. & Scholz, F.J. (1988) Algorithm for the detection of fine clustered calcifications on film mammograms. Radiology 169: p. 333-337.

Feig, S.A., (1988) Decreased breast cancer mortality through mammographic screening: Results of clinical trails. Radiology, 167: p. 659-665.

Hollingsworth, A.B., Taylor, L.D., & Rhodes, D.C. (1993) Establishing a histologic basis for false-negative mammograms. American Journal of Surgery, 166(6): p. 643-648.

Kopans, D., (1992) Detecting Breast Cancer Not Visible by Mammography. JNCI, 84(5): p. 745-747.

Kopans, D.B., (1984) Early breast cancer detection using techniques other than mammography. Am. J. Roentgenol. 143: p. 465-468.

Lefebvre, F., Benali, H., & Kahn, E. (1992) Fractal analysis of clustered microcalcifications in digital mammograms. Acta. Stereol. 11: p. 611-616.

Lefebrvre, F., Benali, H., Gilles, R., Kahn, E., & DiPaola, R., (1995) A fractal approach to the segmentation of microcalcifications in digital mammograms. Med Phys. p. 381-391.

Maidiment, A.D.A., Fahrig, R., & Yaffe, M.J. (1993) Dynamic range requirements in digital

mammography. Med. Phys. 20: p. 1621-1633.
Moskowitz, M. (1984) Mammography to screen asymptomatic women for breast cancer. Am. J. Roentgenol. 143: p. 457-459.
Moskowitz, M., Gartside, P. & McLaughlin, C. (1980) Mammographic patterns as markers for high-risk benign breast disease and incident cancers. Radiology, . 134(2): p. 293-5.
Myers, L.E., McLelland, R., Stricker, C.X., Feig, S.A., Martin, J.E., Moskowitz, M., & N ielsen, M.E.J.(1983). Reproducibility of Mammographic Classifications. AJR, 141: p 445-450.
Neitzel, T.J. (1994) Discernible gray levels and digitization requirements in digital mammography. Med Phys. 21: p. 1213-1214.
Nishikawa, R.M. et al., (1993)Computer-aided detection and diagnosis of masses and clustered microcalcifications from digital mammograms. Proc. SPIE 1905: p. 422-431 .
Oza, A.M. and Boyd, N.F.1993.Mammographic parenchymal patterns: a marker of breast cancer risk. [Review]. Epidemiologic Reviews, 15(1): p. 2507-2517.
Priebe, C.E., Solka, et al., (1994) The application of fractal analysis to mammographic tissue classification Cancer Letters. 77(2-3): p. 183-189.
Ruttimann, E., Webber, R.L., & Hazelrig, J.B. (1992) Fractal dimension from radiographs of peridental alveolar bone. Oral Surg Oral Med Oral Pathology 74: p. 98-109.
Sickles, E.A., (1986) Mammographic features of 300 consecutive nonpalpable cancers. Am. J. Roentgenol. 146: p. 661-663.
Tabar, L., Fagerburg, G., Duffy, S.W., Day, N.E., Gad, A., & Grontoft, O. (1992) Update to the Swedish two-country program of mammographic screening for breast cancer. Radiol.Clin. N. America. 30: p. 187-210.
Taylor, P., Haynal, S., Dilhuydy, M.H. & Barreau, B., (1994) Measuring image texture to separate difficult from easy mammograms. Brit. J. of Radiology 67: p. 456-463.
Warner, E., Lockwood, G., Trichler, D., & Boyd, N.F. (1992)The risk of breast cancer associated with mammographic parenchymal patterns: a meta-analysis of the published literature to examine the effect of method of classification. Cancer Detection & Prevention, 16(1): p. 67-72.
Wolfe, J.N., (1976)Breast patterns as an index of risk for developing breast cancer. American Journal of Roentgenology, . 126(6): p. 1130-7.
Wolfe, J.N., Saftlas, A.F., & Salane, M.(1987) Mammographic parenchymal patterns and quantitative evaluation of mammographic densities: a case-control study. AJR. 148(6): p. 1087-92.
Wu, Y., Doi, K., Giger, L., & Nishikawa, M., (1992) Computerized detection of clustered microcalcifications in digital mammograms: Applications of artificial neural networks. Medical Physics 19: p. 555-560.
Zhang, D., Doi, K., Giger, et al., (1992) Computerized detection of cluster microcalcification in digital mammograms: application of artificial neural networks. Med.Phys. 19: p. 555-560.
Zheng, B., Chang, Y.H., Staiger, M., Good, W. & Gur. D (1995) Computer-aided detection in digitized mammograms.Acad. Radiol 2: p. 655-662.

EARLY DETECTION OF BREAST CANCER WITH ULTRASOUND MAMMOGRAPHY

Final report under USArmy Med. R&D.Com. grant DAMD17-93-J-3014.
B.D.Steinberg, Q.Zhu, J.Schwartz, D.Carlson
Valley Forge Research Center
Moore School of Electrical Enginering
University of Pennsylvania

1. INTRODUCTION

The long term objective of the project is ultrasonic echo-scanning demonstration of the detection and diagnosis of small breast tumors of a few mm (~ 2 mm) in size. Small tumor detection requires large (~f/1), 2-D transducer array (5-10cm) to achieve the high lateral resolution. Imaging from so large an aperture suffers wavefront aberration. The wavefront aberration problems inside the female breast are caused by distortion sources of two distinct types, isotropic scattering and nonisotropic multipath caused by refraction and/or reflection. Scattering diminishes contrast resolution (CR), and multipath create false targets or ghost image artifacts. Both reduce CR in image. We seek -60 to -70 dB CR for echo imaging so as to prevent contamination of otherwise black cysts with scattered and/or refracted echo energy and thereby to cause them to look like speckled tumors.

The tools that we proposed to investigate were adaptive signal processing methods for wavefront distortion compensation. In addition, we also proposed to study large aperture design principles for next generation high resolution ultrasound breast scanner. In the last year, we found that applying a time delay type algorithm developed by Flax and O'Donnell (1988) to *in vitro* 2-D breast data and the algorithm has suppressed scattered energy and folded it into the target image, increasing CR by 10-20 dB (Hinkelman et al, 1995, Zhu and Steinberg, 1994). Such adaptive algorithms have been developed in many fields in the last 20 years (optics, Muller, 1974; radar, Steinberg, 1981; radio astronomy, Cornwell, 1989; ultrasound, Flax and O'Donnell, 1988, Nock *et al.* ,1989, Fink, 1992). These are global algorithms that correct time delay errors in wavefronts caused by inhomogeneous tissue and leave the wavefront amplitude distortion intact. This type of algorithm is well understood and can be applied to echoscanners with modest success. Recently, we have had a leap in understanding as to how to properly treat the wavefront amplitude distortion and multipath interference problems. Our newest Toward Inverse Filter (TIF) approach, submitted for publication (Appendix A), has shown 6-10 dB improvement in CR more than phase conjugation, the best phase correction procedure. Our spatial location diversity and coherent CLEAN approach, though preliminary, increases CR by ~7 dB (Appendix G).

2. SUMMARY OF THE ACHIEVEMENTS

There were four major tasks in the proposal. These items were either completed or are in progress. Publications resulting from this work are referenced in subpar. 1-4 immediately below.

1. Analyze and evaluate 1-D *in vivo* breast wavefront data from a point source measured with a 10-cm 1-D linear array. Extract statistical information about waveform

distortion from the data. This information is valuable for the design of stronger wavefront compensation algorithms.

The 1-D data had been taken at Hosp. Univ. Pennsylvania (HUP) on an earlier Commonwealth of Pa. grant. 44 asymptomatic women who had x-ray mammography were studied. They were divided into three approximately equal size groups - premenopausal dense breasts, premenopausal fatty and postmenopausal. Propagation path in tissue was 12 cm. Frequencies were 3 and 4 MHz. Waveforms were wideband (to emulate echo) and narrowband (to avoid frequency selective phenomena). Statistics were obtained and published on wavefront amplitude distribution, correlation distance and image sidelobe levels caused by wavefront distortion [1,2,3,4].

2. Extend measurement capability to 2-D. Obtain 2-D breast data. Analyze as in item 1.

2-D breast data obtained and analyzed, from collaboration with URochester group [5, 6]. In addition to data analysis, we also completed a theoretical scattering model [7]. It predicts halo around target, calculates halo width and intensity, calculates loss in target contrast and dynamic range vs array size, frequency, propagation depth in tissue, phase or time delay variance in tissue, scatterer size, correlation distance. Compares favorably with reported experimental data. The model can be used to guide the design of high resolution ultrasound systems.

3. Test existing phase deaberration algorithms. Determine suitability to high resolution imaging in the breast. Develop stronger wavefront compensation algorithms as needed to the extent possible.

Existing phase deaberration algorithms were tested and compared both theoretically and experimentally upon 2-D measurement data (dominant scatterer (Steinberg, 1981)/ time reversal mirror (Fink, 1993), time delay correction (Flax and O'Donnell, 1988, Nock, et al., 1989), backpropagation plus time delay (Liu and Waag, 1994)) [6,8]. Two types of stronger wavefront compensation algorithms have been developed. These are:

a. Toward Inverse Filtering Approach

2-D data analysis and 2-D algorithmic studies indicate that ultrasonic wavefront distortion inside the female breast falls into two categories, incoherent scattering and coherent multipath. Scattering reduces target strength, broadens image lobe and lowers the image contrast while refraction creates coherent multipath interference that produces false targets or ghost artifacts in the image [6,8]. Time-delay type compensation algorithms are useful to minimize scattered energy and to improve image contrast to a large extent (15 dB) [5,6]. Further improvement of contrast resolution requires compensation algorithms that can compensate wavefront amplitude distortion and remove false targets. A new approach, Toward Inverse Filtering, which is designed to solve scattering problem, is developed and experimentally demonstrated using 2-D *in vitro* measurement data [6,8]. Contrast resolution has been improved 6 - 10 dB more than the best phase deaberration procedure (phase conjugation) at the aperture.

b. Multipath Identification and Cancellation Procedure

Multipath interference is a much more difficult problem than scattering. Because it is not a stationary, stochastic process, two distinct steps are required to deaberrate refraction-contaminated image. It is first necessary to recognize which target is the true target and which is the false one caused by interference. In [9] we demonstrate that when a cluster of true and false targets is imaged from several different array locations the true target remains in position and changes very little in size and shape. The images of false targets, on the

other hand, are highly sensitive to the direction from which they are viewed. Therefore, they change sufficiently in location, size and shape to classify them as false. In this way the recognition problem is solved. The second key problem is the cancellation of the multipath arrivals. In [9], we show that coherent CLEAN deconvolution technique can be used as a tool to solve the second problem; a single pole cancellor has offered average of 7 dB improvement in target dynamic range. Sophisticated cancellations, which are now being studied, are expected to offer more. These results, though preliminary, lead to considerable optimism that this approach may lead to the solution of the second problem.

4. Design and test 2-D large acoustic transducers for higher resolution imaging.

a. 2-D Acoustic Array Design

Dramatically reducing the number of transducer elements in a large 2-D array, called element thinning, is essential for designing a practical 2-D transducer array. Analysis revealed that by using the ultrawideband (UWB) property of this array, very thin high resolution arrays can be built. Several groups have studied random, sparse, two-dimensional ultrasonic arrays (Turnbull *et al*, 1992, Cassereau *et al* 1992, Davidsen*et al*, 1994). They chose a random allocation of elements in order to avoid the grating lobes of a periodically thinned array. Consequently, the resulting side energy of the radiation field is much higher than that of a filled array, as predicted by random array theory. These groups did not consider the ultrawideband nature of currently available transducers in their array design. The distribution of sidelobe energy from an UWB array is very different from a conventional narrowband (NB) array. Due to the UWB nature of the pulse, the radiated waveform from UWB arrays varies in time which is not the case in NB arrays. As a result, the waveform has an extra dimension with respect to NB radiation fields across which undesired side energy can be distributed. We have found that UWB arrays can be highly thinned and achieve a much lower side energy level than NB arrays.

Our theory and simulations show that when UWB arrays are highly thinned, there exist regions of the radiation fields where there is no interference. NB array analysis is based on the assumption that the entire radiated field has interference; therefore, conventional NB analysis does not apply in highly thinned UWB arrays. The analysis to date established a method for characterizing the radiation from highly thinned UWB one- and two-dimensional arrays. This method simplified the radiation field by analyzing its interfering and a non-interfering regions separately. The results showed that, contrary to conventional wisdom, a periodic array is preferred over a random array. Furthermore, to achieve the same high resolution and low side radiation level, the highly thinned periodic UWB array is capable of reducing the number of elements required in a conventional filled array to approximately the square root of that number. We call such an array a $\sqrt{N}$ array.

As a consequence of element thinning, there is a loss in signal-to-noise because of the loss in aperture area. A parametric relation was derived which gives the minimum number of elements required to insure an adequate signal-to-noise ratio. Theoretically, it can be shown that the $\sqrt{N}$ array is capable of achieving a sufficient signal-to-noise ratio for pulse-echo ultrasonic imaging.

b. Equipment for Experiment Program

The ultrasound laboratory is fully operational and is used daily in support of the experimental program. The facility includes a water tank test chamber that is designed for 3-D synthetic aperture imaging with arbitrary transducer array configurations within a 15-cm cube. A three-axis micro-positioner table with linear encoders (purchased from New England Affiliated Technology) provides for the control of element position accuracy within 3 microns. In a typical experiment, a fixed hemispherical transducer radiates a short pulse (500 nsec) at 3.75 MHz, and a 0.6 mm hydrophone receives the resulting waveform

at each desired measurement position. Each received waveform is sampled well above the Nyquist rate, displayed and digitized by a HP54120T sampling oscilloscope, and stored in a desktop computer. The entire experiment is under preprogrammed computer control. The output data set includes a received waveform from each receiving element-position. Each data set is then operated upon by relevent software, i.e., imaging, Fourier transform, correlation, etc.

3. CONCLUSION

Adaptive wavefront compensation is a useful tool to increase CR for ultrasonic breast imaging and the total CR improvement in point source image is about 25 dB. The next step will be the careful evaluation of these methods using 2-D large aperture pulse-echo system upon *in vitro* samples and *in vivo* volunteers.

Simulations show that highly thinned UWB arrays are able to achieve high resolution and a low side radiation level while maintaining a sufficient signal-to-noise level. A periodic configuration of elements gives a lower side radiation level than a random array and is able to reduce the number of elements conventionally required by a filled array to about the square root of that number. The next step in the array design is to experimentally verify the properties of this $\sqrt{N}$ array in our ultrasonic experimental system.

4. PUBLICATIONS

[1]. Zhu, Q. and Steinberg, B. D., "Wavefront Amplitude Distribution in the Female Breast," J. Acoust. Soc. Am. (46) 1-9 (1994).

[2]. Zhu, Q., Steinberg, B. D. and Arenson, R, "Correlation Distance Measurements of the Female Breast," J. Acoust. Soc. Am, (98) 694-705 (1995).

[3]. Zhu, Q. and Steinberg, B. D., "Wavefront Amplitude Distortion and Image Sidelobe Levels - Part I: Theory and Computer Simulation," IEEE Transactions on Ultrasonic, Ferroelectrics and Frequency Control (40) 747-753 (1993).

[4]. Zhu, Q., Steinberg, B. D. and Arenson, R., "Wavefront Amplitude Distortion and Image Sidelobe Levels -Part II: In Vivo Experiments," IEEE Transactions on Ultrasonic, Ferroelectrics and Frequency Control (40) 754-761 (1993).

[5]. Hinkelman, L. M., Liu, D-L., Zhu, Q., Steinberg, B. D. and Waag, R. C., "Measurement and Correction of Ultrasonic Pulse Distortion Produced by the Human Breast," J. Acoust. Soc. Am. (97) 1958-1969 (1995).

[6]. Zhu, Q., Steinberg, B.D., Hinkelman, L. M., and Waag, R. C., "Deaberration of Incoherent Wavefront Distortion: An Approach Toward Inverse Filtering,", submitted to IEEE Transactions on Ultrasonic, Ferroelectrics and Frequency Control (Jan. 1996).

[7]. B.D.Steinberg, "Scattering from a Multiple Random Phase Screen Model of a Random Inhomogeneous Medium," submitted to JASA (Feb. 1995).

[8]. Zhu, Q. and Steinberg, B.D., "Modelling and Correction of Incoherent Wavefront Distortion" (Invited paper) Submitted to I'nal. J. Sci. Tech. Imaging, Wiley (Sept., 1995).

[9]. Zhu, Q. and Steinberg, B.D., "Correction of Multipath Interference by Spatial Location Diversity and Coherent CLEAN," Proc. IEEE Ultrasonic Symp. (1995).

[10]. Schwartz, J. L. and B. D. Steinberg, "The Characteristics of Interference Patterns Produced by Ultra-Wideband Arrays," URSI, Nat'l Radio Sci. Meeting, January 1995.

[11]. Schwartz, J. L. and B.D. Steinberg, "Highly-Thinned, Two-Dimensional Arrays," Ultrasound Deaberration Workshop, Wash., DC, June 1995.

[12]. Schwartz, J. L. and B.D. Steinberg, "Highly-Thinned Arrays for Ultrasonic Imaging," accepted to the AIUM conference in March 1996 in New York.

[13] Schwartz, J.L. and B.D. Steinberg, "UltraSparse, Ultrawideband, Phased Arrays," submitted to the IEEE AP-S and URSI Radio Science Meeting in July 1996 in Baltimore.

REFERENCES

Cassereau, D., N. Chakroun, F. Wu, M. Fink and F. Datchi, "Synthesis of a specific wavefront using 2D full and sparse arrays," 1992 IEEE Ultrasonics Symposium.

Cornwell, T. J., "The Application of Closure Phase to Astronomical Imaging," Science **245**, 4915 (1989).

Davidsen, R. E., J.A. Jensen, and S. W. Smith,"Two-Dimensional Random Arrays for Real Time Volumetric Imaging," Ultrasonic Imaging **16**, 143-163, 1994.

Fink, M., "Time reversal of ultrasonic fields – part I: basic principles," IEEE Trans. Ultrason. Ferroelec. Freq. Contr., vol. 39, pp. 555-566, 1992.

Flax, S. W. and O'Donnell, M. "Phase Aberration Correction using Signals from Point Reflectors and Diffuse Scatterers: Measurements," IEEE Trans. Ultrason. Ferroelec. Freq. Cont., **35**(6):768-774, Nov. 1988.

Hinkleman, L.M., Liu, D-L., Waag, R.C., Q. Zhu and B.D.Steinberg, "Measurement and correction of ultrasonic pulse distortion produced by the human breast," JASA (97) No.3, 1958-1969 (1995).

Liu D-L and Waag, R.C., "Correction of Ultrasonic Wavefront Distortion Using Backpropagation and Reference Waveform Method for Time-shift Compensation, " J. Acoust. Soc. Am. 96, 649-660 (1994).

Muller R.A., and Buffington, A., "Real-Time Correction of Atmospherically Degraded Telescope Images through Image Sharpening," J.Opt. Soc. Am., **64**(9) 1200-1210 (September 1974).

Nock, L., Trahey, G. E., and Smith, S.W., "Phase Aberration Correction in Medical Ultrasound Using Speckle Brightness as a Quality Factor," J. Acoust. Soc. Am., **85**(5) 1819-1833 (1989).

Steinberg,B.D, "Radar Imaging from a Distorted Array: The Radio Camera Algorithm and Experiments," IEEE. Trans. Antennas Propag., **AP-29**(5) 740-748 (Sept. 1981).

Turnbull, D. H., P. Lum, A. K. Kerr and F. S. Foster, "Simulation of B-scan images from two-dimensional transducer arrays: Part I:- Methods and quantitative contrast measurements," Ultrasonic Imaging **14**, 323-343. 1992.

Zhu, Q. and Steinberg, B. D., "Modeling, Measurement and Correction of Wavefront Distortion Produced By Breast Specimens," Proc. IEEE Int'l Symp. Ultrason. Ferroelec. Freq. Cont., Cannes, Nov. 1994.

ADDENDUM TO GRANT NUMBER DAMD 17-93-J-3014

Title: Early Detection of Breast Cancer on Mammograms using: Perceptual Feedback, Computer Processed Image and Ultrasound

Principal Investigator: Peter Bloch, Ph.D.

Report Date: May 30 1996

Type of Report: Report for the period 12/30/95-4/30/96

The grant was extended 4 months with no additional funds. The extension permitted us to further study digital processing of mammography images to improve observer performance in identifying microcalcification and masses.

During this extension period techniques were explored to use the digital mammograms more readily in a clinical setting. The digitized high resolution mammograms are large files typically 30-50 megabytes. Transferring and computer processing these files, which takes approximately 5-10 minutes, is too long for routine clinical use.

We investigated reducing the mammogram file size by decreasing the number of bits per pixel. The digitized images are obtained at 16 bits/pixel. Reducing to 8 bits/pixel decreased the observers ability to detect the boundary of the breast on the mammogram. In addition, when the number of bits/pixel was reduced from 16 to 14 bits the computer-assisted identification of microcalcifications on a mammogram was adversely affected. The reduction in the number of bits/pixel, changed the calculated regional distribution of fractal dimension and entropy within the mammogram. The fractal dimension distribution within the mammogram image (see Final Progress report) became a less sensitive indicator of the presence of a microcalcification when the number of bits/pixel was reduced.

The results of these studies show the importance of maintaining in the digital image the wide gray scale or latitude of the original film-screen mammogram.

We are continuing to explore other techniques (without external funding) to reduce the digitized mammography file size. Cropping the image to include only the breast tissue significantly decreases the file size, typically 30-50%. The automatic detection of the boundary of the breast on the mammogram that was developed during the course of the grant will be employed for automatic cropping of the image.

Recently, we have been made available the high resolution digitized mammography data-base and the algorithms to computer process these images to the National Information Display Laboratory (NIDL) at the David Sarnoff Research Center, in Princeton, N.J.

Previously, NIDL developed techniques for analyzing aerial photographs. They are now interested in applying these techniques for detection of lesions on mammograms. The collaboration between the Univ. of Pennsylvania and NIDL is in keeping with the Public Health Service Women's Health program of "Missiles to Mammogram" initiatives. The mammography developments at our institution in digital mammography and breast cancer detection with magnetic resonance imaging and spectroscopy, both supported with DAMD funds, are being correlated using hardware and software at NIDL. The combination of the two modalities should provide additional information that could significantly improve breast cancer diagnoses, especially in difficult to read mammograms of dense breast tissue.

Our recent developments in digital mammography has also result in a potential collaborative program with a commercial company to explore using solid-state digitally acquired mammograms in a clinical setting. The direct digital acquisition of a mammogram may be essential for wide spread introduction of computer-assisted diagnosis of mammograms. The feature extraction algorithms that were developed for film-screen mammograms can be employed with these digitally acquired images during the period of the grant.